PFC/JA-93-15

Linear and Nonlinear Analysis of the Cyclotron Two-Stream Instability

C. Chen, G. Bekefi and W. Hu

July, 1993

Plasma Fusion Center
and
Department of Physics
Massachusetts Institute of Technology
Cambridge, MA 02139

Submitted for publication in Physics of Fluids B. This work was supported in part by SDIO/IST under the management of the Army Research Laboratory and in part by the Air Force Office of Scientific Research.

Linear and Nonlinear Analysis of the Cyclotron Two-Stream Instability

Chiping Chen, George Bekefi, and Wen Hu
Plasma Fusion Center,
Research Laboratory of Electronics, and
Department of Physics
Massachusetts Institute of Technology
Cambridge, Massachusetts 02139

ABSTRACT

A two-dimensional, self-consistent, nonlinear model is used to determine the growth rate and saturation level of the cyclotron two-stream instability for two weakly relativistic electron beams co-propagating along a uniform magnetic field with an inverted population in the perpendicular momentum. This instability has been proposed recently as the basis for a double-stream cyclotron maser. Good agreement is found between the dispersion analysis and computer simulations in the linear regime. The effect of axial momentum spread on the instability is investigated. It is shown that the cyclotron two-stream instability is primarily electrostatic, which calls for further exploration of an effective input and output coupling scheme for the maser.

PACS numbers: 41.60.Cr, 41.75.Ht, 52.75.Ms, 52.25.Wz

I. INTRODUCTION

The exploration of novel mechanisms of generating millimeter waves with relativistic electron beams has been pursued vigorously in recent years. The sought-after operating regime of millimeter wave sources of particular interest would require a mildly relativistic ($\leq$ 100 kV) electron beam and moderate magnetic field ($\leq$ 1 kG). The *double-stream cyclotron maser* [1], which utilizes two mildly relativistic electron beams co-propagating along an applied uniform magnetic field with an inverted population in the perpendicular momentum, is one of the proposed mechanisms that satisfies this requirement.

The operating principle of the double-stream cyclotron maser [1] is based on the unstable interaction of the *fast* cyclotron space-charge wave on one electron beam and the *slow* cyclotron space-charge wave on the other electron beam. Such an unstable interaction, which we refer to as the *cyclotron two-stream instability*, leads to the stimulated bunching of the gyrophases of the electrons relative to the wave phase. The cyclotron two-stream instability belongs to the class of multiple species, quasi-electrostatic streaming instabilities well known in plasma physics. Figure 1 shows a schematic dispersion diagram for such a two-stream system, where there are an infinite number of unstable regions appearing in the vicinities of the intersections of the cyclotron modes of one beam with those of the other beam. Because the resonant frequency of the cyclotron two-stream interaction is proportional to the cyclotron frequency and is *inversely* proportional to the difference in the axial velocities of the beams, the double-stream cyclotron maser can operate at high frequencies without the need of either high beam voltage or high magnetic field.

In this paper, we present a two-dimensional, self-consistent, fully nonlinear wave-particle model for studies of the feasibility of the double-stream cyclotron maser in particular and the cyclotron two-stream instability in general. The linear and nonlinear coupling of axisymmetric cyclotron space-charge waves on two weakly relativistic electron

beams co-propagating in a uniform magnetic field is investigated in cylindrical geometry. When the Doppler shift in frequency is much greater than the cyclotron frequency, the coupling is shown to be primarily *electrostatic*, which differs qualitatively from an electromagnetic type of coupling considered previously [2]. The linearized equations of motion in the present wave-particle model are used to derive a dispersion relation for the electrostatic coupling, which is in agreement with what was derived previously [3] using kinetic theory. The linear stability properties are analyzed. It is found that, like the conventional cyclotron autoresonance maser (CARM) [4],[5], the instability growth rate decreases rapidly with increasing axial velocity spread (i.e., axial beam temperature) within each electron beam. Good agreement is found between the stability analysis and computer simulations in the linear regime. The saturation level of the instability is obtained from simulations for parameter regimes of experimental interest.

The cyclotron two-stream instability is also expected to occur in space plasmas where electrons and ions may stream along a magnetic field with an inverted population in the perpendicular momentum. The model presented in this paper can be generalized to describe the dynamical processes involving such electrons and ions. However, this is beyond the scope of the present paper.

II. THE MATHEMATICAL FORMULATION

We consider two concentric annular beams of electrons gyrating, and co-propagating axially, in an applied uniform magnetic field $B_0\vec{e}_z$ (Fig. 2). The axes of the beam annuli coincide with that of a perfectly conducting, cylindrical waveguide through which the electron beams propagate. Assuming the equilibrium self-electric and self-magnetic fields of the beams to be negligibly small, we describe the unperturbed beams by the following equilibrium distribution function

$$f_0(\vec{x},\vec{p}) = \sum_{\alpha=1,2} f_{0\alpha}(\vec{x},\vec{p}) = \sum_{\alpha=1,2} \frac{I_\alpha}{eV_\alpha} G_\alpha(r_g) F_\alpha(p_\perp, p_z) \ , \tag{1}$$

with $2\pi \int G_\alpha(r_g) r_g dr_g = 1$ and $2\pi \int F_\alpha(p_\perp, p_z) p_\perp dp_\perp dp_z = 1$. In Eq. (1), $-e$ is the electron charge, p_z and $p_\perp = (p_x^2 + p_y^2)^{1/2}$ are the electron axial and perpendicular momentum components, respectively, r_g is the electron guiding-center radius, and I_α and $V_\alpha = \int v_z F_\alpha d^3p$ are the current and average axial velocity of beam α, respectively. Note that the variables r_g, p_z, and $p_\perp$ are the constants of the unperturbed single electron motion in the uniform magnetic field $B_0\vec{e}_z$ and therefore, the equilibrium distribution function f_0 solves for the zeroth-order Vlasov equation.

To derive a complete set of ordinary differential equations describing the self-consistent, slowly varying, axial evolution of cyclotron space-charge waves in a single-frequency, stationary-state, double-stream cyclotron maser amplifier, we express the axisymmetric wave fields in terms of a vector potential of the form

$$\vec{A}(r, z, t) = A_z(r, z, t)\vec{e}_z \ , \tag{2}$$

where the axial component of the vector potential is defined by

$$A_z(r, z, t) = -\frac{i}{2} \sum_{n=1}^{\infty} A_n(z) C_{\perp n} J_0(k_{\perp n} r) \exp\{i[\int_0^z k_{zn}(z')dz' - \omega t]\} + \text{c.c} \tag{3}$$

and the transverse components $A_r(r, z, t)$ and $A_\theta(r, z, t)$ are ignored. The electric and magnetic field perturbations are then uniquely determined from Eq. (3) using the Lorentz gauge condition. In the regime considered in the present analysis, the neglect of the transverse components of the vector potential is justified because the coupling is primarily through electrostatic forces due to a large Doppler upshift of the cyclotron frequency.

In Eq. (3), the index n designates a TM_{0n} type of transverse-magnetic mode; and $J_0(x)$ is the zeroth-order Bessel function of the first kind. The transverse field profile $J_0(k_{\perp n} r)$ corresponds to that of the vacuum TM_{0n} mode, provided that the boundary condition $J_0(k_{\perp n} b) = 0$ is satisfied. Here, b is the waveguide radius, $k_{\perp n} = \mu_n / b$, μ_n is the n-th zero of $J_0(x)$, and

$$C_{\perp n} = \frac{k_{\perp n}}{\pi^{1/2} \mu_n |J_0'(\mu_n)|} \tag{4}$$

is a normalization constant. In the present model, the coupling between the wave fields and the beam density and current perturbations is described by the slowly varying wave amplitudes $A_n(z)$ and the slowly varying axial wave numbers $k_{zn}(z)$. It should be noted that the axisymmetric vector potential in Eq. (3) is expressed as a superposition of a complete set of the vacuum TM_{0n} modes and thereby allows us to treat both electrostatic waves and electromagnetic waves on the same footing. Detailed discussions of this expansion technique can be found in references [6] and [7].

From the Lorentz and Maxwell equations, it can be shown that a complete set of normalized ordinary differential equations governing the double-stream cyclotron maser amplifier is given approximately by

$$\frac{d\psi_{nl}}{d\hat{z}} = \hat{k}_{zn}(\hat{z}) - \frac{\gamma}{\hat{p}_z} + \frac{l\hat{\Omega}_c}{\hat{p}_z} , \tag{5}$$

$$\frac{d\gamma}{d\hat{z}} = \sum_{n=1}^{\infty}\sum_{l=-\infty}^{\infty}\frac{X_{nl}}{\hat{k}_{\perp n}}\left\{-\left[(1-\hat{k}_{zn}^2)a_n + \frac{d^2a_n}{d\hat{z}^2}\right]\cos\psi_{nl} + \left(\frac{d\hat{k}_{zn}}{d\hat{z}}a_n + 2\hat{k}_{zn}\frac{da_n}{d\hat{z}}\right)\sin\psi_{nl}\right\} , \tag{6}$$

$$\hat{p}_\perp \cong \text{const} , \tag{7}$$

and

$$\frac{d^2a_n}{d\hat{z}^2} + (1-\hat{k}_{zn}^2-\hat{k}_{\perp n}^2)a_n + i\left(2\hat{k}_{zn}\frac{da_n}{d\hat{z}} + a_n\frac{d\hat{k}_{zn}}{d\hat{z}}\right) = i\sum_{l=-\infty}^{\infty}\sum_{\alpha=1,2} g_{n\alpha}\langle X_{nl}\exp(-i\psi_{nl})\rangle_\alpha . \tag{8}$$

The procedure of deriving Eqs. (5)-(8) can be found in [6].

Equations (5)-(7) describe the dynamics of an individual beam electron. In our simulations, we solve numerically $6N$ of such equations of motion for N macroparticles representing the electrons of each beam, where $N = 1024$ is typical. The phase ψ_{nl} is defined by

$$\psi_{nl}(z,\phi,\theta_g,t) = \int_0^z k_{zn}(z')dz' - \omega t + l\tan^{-1}(p_y/p_x) - l\theta_g + l\pi/2 \tag{9}$$

and represents the l-th harmonic gyrophase of the electron relative to the phase of the n-th mode, where $\theta_g \cong$ const is the polar angle of the guiding center of the electron.

$X_{nl}(r_g, r_L) = J_l(k_{\perp n} r_g) J_l(k_{\perp n} r_L)$ is a geometric factor and r_L is the Larmor radius of the electron. The normalization is such that $\hat{z} = \omega z/c$, $\hat{k}_{zn} = ck_{zn}/\omega$, $\hat{p}_\perp = p_\perp/mc$, $\hat{p}_z = p_z/mc$, $\hat{\Omega}_c = \Omega_c/\omega = eB_0/mc\omega$, etc., (which is equivalent to setting $m = e = c = \omega = 1$, where m is the electron rest mass, and c, the speed of light in vacuum).

Equation (8) describes the self-consistent evolution of both the normalized wave amplitude $a_n(\hat{z})$ and axial wave number $\hat{k}_{zn}(\hat{z})$. The dimensionless coupling constant in Eq. (8) is defined by

$$g_{n\alpha} = 8\pi \left(\frac{ck_{\perp n}}{\omega}\right)^3 \left(\frac{C_{\perp n}}{k_{\perp n}}\right)^2 \left(\frac{I_\alpha}{I_A}\right) , \tag{10}$$

where $I_A = mc^3/e = 17$ kA is proportional to the Alfvén current. The notation $\langle \chi \rangle_\alpha = N^{-1} \sum_{j=1}^{N} \chi_j$ denotes the ensemble average over the particle distribution of beam α.

The average electromagnetic power flow (i.e., Poynting flux) through the waveguide cross section at the axial distance z is given by

$$P(z) = \sum_{n=1}^{\infty} P_n(z) , \tag{11}$$

where

$$P_n(z) = \frac{P_0}{8\pi} \frac{ck_{zn}(z)}{\omega} \left(\frac{\omega}{ck_{\perp n}}\right)^2 \left(\frac{k_{\perp n}}{C_{\perp n}}\right)^2 a_n^2(z) \tag{12}$$

is the power contributed by the n-th mode and $P_0 = m^2c^5/e^2 = 8.7$ GW. Moreover, the average rf e-beam power flow is given by

$$P_b = \sum_{\alpha=1,2} P_0 \left(\frac{I_\alpha}{I_A}\right) (\langle \gamma \rangle_\alpha - 1) \tag{13}$$

From Eqs. (6), (8), and (10)-(13), it follows that the total rf power is conserved, i.e., $P(z) + P_b(z) = \text{const.}$

The mathematical formulation presented above is readily used to examine the stability properties and saturation levels of cyclotron space-charge waves on two relativistic electron beams co-propagating in a finite magnetic field. In principle, the present formulation is also applicable in regimes where the gyromotion of the beam electrons is

negligible, (i.e., $B_0 \to \infty$), as in the two-stream relativistic klystron amplifier [8],[9] configuration. The latter case is obtained by setting the cyclotron harmonic number l equal to zero for each beam. In the remainder of this paper, we present results of a single-mode analysis in which we let n be a single integer but allow the cyclotron harmonic number l to assume integers $0, \pm 1, \pm 2, \cdots$.

III. ELECTROSTATIC DISPERSION RELATION

In the small-signal regime, we can linearize Eqs. (5)-(8) and derive a dispersion relation. Making an electrostatic approximation ($k_z^2 + k_\perp^2 \gg \omega^2/c^2$), and choosing the equilibrium distribution function in Eq. (1) with

$$G_\alpha(r_g) = \frac{1}{2\pi r_{g\alpha}} \delta(r_g - r_{g\alpha}) \tag{14}$$

and

$$F_\alpha(p_\perp, p_z) = \frac{1}{2\pi p_{\perp\alpha}} \delta(p_\perp - p_{\perp\alpha}) \delta(p_z - p_{z\alpha}) \ , \tag{15}$$

it is readily shown that the dispersion relation for the n-th mode can be expressed as

$$D_n^L(\omega, k_z) = 1 - \sum_{l=-\infty}^{\infty} \sum_{\alpha=1,2} \frac{\epsilon_{ln\alpha} c^2 k_{\perp n}^2}{(\omega - k_z v_{z\alpha} - l\Omega_c/\gamma_\alpha)^2} = 0 \ . \tag{16}$$

In Eq. (16), we have neglected terms of order $(\omega - k_z v_{z\alpha} - l\Omega_c/\gamma_\alpha)^{-1}$. Neglect of this term is well justified whenever $k_\perp/k_z \ll 1$, as is the case of present interest. The normalized coupling constant is defined by

$$\epsilon_{ln\alpha} = \frac{4}{\gamma_\alpha \beta_{z\alpha} \gamma_{z\alpha}^2} \left(\frac{I_\alpha}{I_A}\right) \left[\frac{J_l(k_{\perp n} r_{g\alpha}) J_l(k_{\perp n} r_{L\alpha})}{k_{\perp n} b J_0'(k_{\perp n} b)}\right]^2 \ , \tag{17}$$

which is related to $g_{n\alpha}$ defined in Eq. (10). Here, $\gamma_\alpha = (1 + \hat{p}_{z\alpha}^2 + \hat{p}_{\perp\alpha}^2)^{1/2}$, $\beta_{z\alpha} = \hat{p}_{z\alpha}/\gamma_\alpha$, $\beta_{\perp\alpha} = \hat{p}_{\perp\alpha}/\gamma_\alpha$, $\gamma_{z\alpha} = (1 - \beta_{z\alpha}^2)^{-1/2}$, $r_{L\alpha} = p_{\perp\alpha}/m\Omega_c$ is the electron Larmor radius of beam α, and $J_l(x)$ is the first-kind Bessel function of order l. The electrostatic dispersion relation (16) has been derived previously [3] in cylindrical geometry using kinetic theory

in the context of a coherently gyrophased electron beam [3],[10], and it is a generalization of a previously obtained dispersion relation [11] for an unbounded system.

IV. NUMERICAL ANALYSIS

We have developed a computer simulation code to integrate Eqs. (5)-(8) numerically. The code has been benchmarked against the linear theory in Sec. III in the small-signal regime. The results of the benchmark simulations are summarized in Figs. 3-5 for the choice of system parameters listed in Table I, where the TM_{02} mode is chosen to maximize the coupling strength.

The (linear) intensity growth rate is plotted in Fig. 3 as a function of frequency. The solid curve is obtained from the electrostatic dispersion relation (16), and the open circles are results from the simulations using Eqs. (5)-(8) which are based on the full Maxwell equation rather than the Poisson equation alone. There are two unstable regions separated at the resonant frequency $f = 34.4$ GHz at which the system is stable. The maximum growth rate is 40 dB/m, which occurs at $f = 26$ and 40 GHz. The fact that there is good agreement between the simulations and the dispersion analysis, as shown in Fig. 3, illustrates that the coupling is indeed primarily electrostatic.

The axial evolution of the normalized wave amplitude is plotted in Fig. 4 for $f = 40$ GHz. At saturation the ac electromagnetic power flow $P_2(z)$ is rather low (< 1 kW) compared with the dc beam power because the wave is primarily electrostatic. Therefore, in order to assure an efficient operation of the maser, an effective input and output coupling scheme is to be sought

The phase space of the electrons, (ψ_{2l}, γ), is shown in Fig. 5 at the initial position $z = 0$ and the final position $z = 200$ cm. In Fig. 5, the open circles represent the macroparticles in beam 1 and the open squares represent the macroparticles in beam 2. At $z = 0$, the gyrophases of the macroparticles in both beams are slightly bunched

relative to the wave phase so that a small wave amplitude can be assigned initially in the simulation. At $z = 200$ cm, the gyrophases of the macroparticles in beam 1 (the circles) are well bunched at the phase $\psi = \psi_{21} \approx 3\pi/2$, whereas the gyrophases of the macroparticles in beam 2 (the squares) are well bunched at the phase $\psi = \psi_{2-1} \approx \pi/2$. One beam bunching out of phase relative to the other beam is a characteristic of the unstable two-stream interaction.

Having found good agreement between theory and simulation for a special choice of the distribution function defined in Eqs. (1), (14), and (15), we have used the code to examine the sensitivity of the growth rate to axial velocity spread within each electron beam. In particular, we have loaded the particles in each beam with a Gaussian axial momentum distribution. The result is shown in Fig. 6, corresponding to the choice of system parameters used in Fig. 3 at the upper maximum gain frequency $f = 40$ GHz. The horizontal axis is a fractional momentum spread defined by $\sigma_{pz}/p_z = \sigma_{pz1}/p_{z1} = \sigma_{pz2}/p_{z2}$, where $\sigma_{pz\alpha}$ is the standard width for beam α. It is seen in Fig. 6 that the growth rate decreases rapidly with increasing spread due to the fact that there is a large Doppler upshift in the frequency. This sensitivity to axial beam temperature is similar to that in the cyclotron autoresonance maser (CARM) [4],[5].

V. CONCLUSION AND DISCUSSION

We presented the first self-consistent nonlinear model for studies of the recently proposed double-stream cyclotron maser in particular and the cyclotron two-stream instability in general. The model was used to analyze the linear and nonlinear coupling of the cyclotron space-charge waves on two weakly relativistic electron beams co-propagating along a uniform magnetic field with an inverted population in the perpendicular momentum. The growth rate and saturation level of the cyclotron two-stream instability were determined from small-signal theory and computer simulations for parameter regimes of

experimental interest. Good agreement was found between linear theory and simulations in the small-signal regime. When the Doppler upshift in frequency is much greater than the cyclotron frequency, the instability growth rate was shown to decrease rapidly with increasing axial velocity spread within each electron beam.

It was shown that the cyclotron two-stream instability is primarily electrostatic. As a result, the electromagnetic energy flux through the waveguide cross section was found to be negligibly small. This calls for further exploration of an efficient input and output coupling scheme for the double-stream cyclotron maser. Such a need for identifying efficient coupling schemes is shared with other slow-wave systems as for example the relativistic klystron.

The numerical calculations performed in this paper assumed for simplicity two overlapping annular relativistic electron beams. However, the theory presented in Sec. II is also applicable to annular beams of different radii. When the radii differ, the gain is reduced, as expected.

ACKNOWLEDGMENTS

This work was supported in part by SDIO/IST under the management of the Army Research Laboratory and in part by the Air Force Office of Scientific Research.

References

[1] G. Bekefi, J. Appl. Phys. **71**, 4128 (1992), and references therein.

[2] C. Wang and S. Liu, Int. J. Electron. **57**, 1191 (1984).

[3] C. Chen, B.G. Danly, G. Shvets, and J.S. Wurtele, IEEE Trans. Plasma Sci. **PS-20**, 149 (1992).

[4] V.L. Bratman, N.S. Ginzburg, G.S. Nusinovich, M.I. Petelin, and P.S. Strelkov, Int. J. Electron. **51**, 541 (1981).

[5] G. Bekefi, A.C. DiRienzo, C. Leibovitch, and B.G. Danly, Appl. Phys. Lett. **54**, 1302 (1989); A.C. DiRienzo, G. Bekefi, C. Chen, and J.S. Wurtele, Phys. Fluids **B3**, 1755 (1991).

[6] C. Chen and J.S. Wurtele, Phys. Rev. Lett. **65**, 3389 (1990); Phys. Fluids **B3**, 2133 (1991).

[7] Y.Y. Lau and D. Chernin, Phys. Fluids **B4**, 3473 (1992).

[8] C. Chen, P. Catravas, and G. Bekefi, Appl. Phys. Lett. **62**, 1579 (1993).

[9] H.S. Uhm, Phys. Fluids. **B5**, in press (1993); H.S. Uhm and C. Chen, submitted to Phys. Fluids. **B** (1993).

[10] A. Fruchtman and L. Friedland, IEEE J. Quantum Electron. **QE-19**, 327 (1983).

[11] A. Bers and C.E. Speck, Massachusetts Institute of Technology, Research Laboratory of Electronics, Quarterly Progress Report **78**, 110 (1965).

Table I. Parameters used for the numerical analysis

Resonant frequency	33.4 GHz
Operating mode	TM_{02} $(n = 2)$
Waveguide radius	2.54 cm
Axial magnetic field	503 G
Beam 1	
Current	100 A
Voltage	137 kV
$v_{\perp 1}/c$	0.2
Guiding-center radius $\langle r_g \rangle_1$	0.88 cm
Harmonic number l	1
Coupling constant ϵ_{121}	1.0×10^{-3}
Beam 2	
Current	100 A
Voltage	163 kV
$v_{\perp 2}/c$	0.2
Guiding-center radius $\langle r_g \rangle_2$	0.88 cm
Harmonic number l	-1
Coupling constant ϵ_{-122}	9.2×10^{-4}

FIGURE CAPTIONS

Fig. 1 Schematic dispersion diagram for a two-stream system in a finite axial magnetic field.

Fig. 2 Schematic of a double-stream cyclotron maser. (a) Cross section of the maser showing the two annular beams and (b) overall view.

Fig. 3 Intensity growth rate as a function of frequency for the choice of system parameters listed in Table I. The solid curve from linear theory [Eq. (16)] and the circles from simulations using Eqs. (5)-(8).

Fig. 4 Normalized wave amplitude as a function of the interaction length z at $f = 40$ GHz for the choice of system parameters listed in Table I.

Fig. 5 Phase space of the beam electrons at (a) $z = 0$ and (b) $z = 200$ cm, corresponding to Fig. 4.

Fig. 6 (a) Intensity growth rate and (b) saturation wave amplitude as a function of the fractional axial momentum spread $\sigma_{pz}/p_z = \sigma_{pz1}/p_{z1} = \sigma_{pz2}/p_{z2}$.

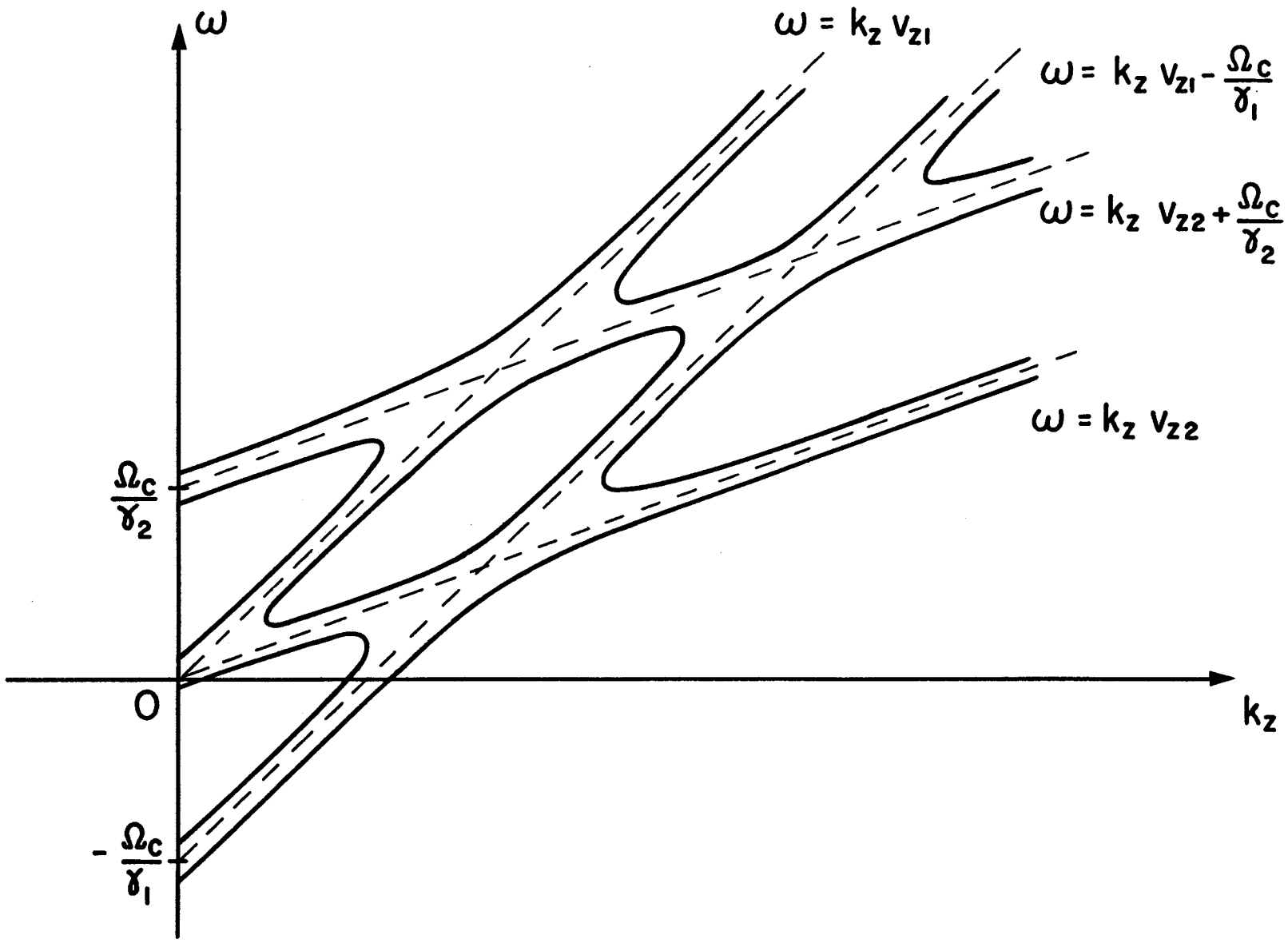
ω
$\omega = k_z v_{z1}$
$\omega = k_z v_{z1} - \frac{\Omega_c}{\gamma_1}$
$\omega = k_z v_{z2} + \frac{\Omega_c}{\gamma_2}$
$\omega = k_z v_{z2}$
$\frac{\Omega_c}{\gamma_2}$
0
$-\frac{\Omega_c}{\gamma_1}$
k_z

Figure 1

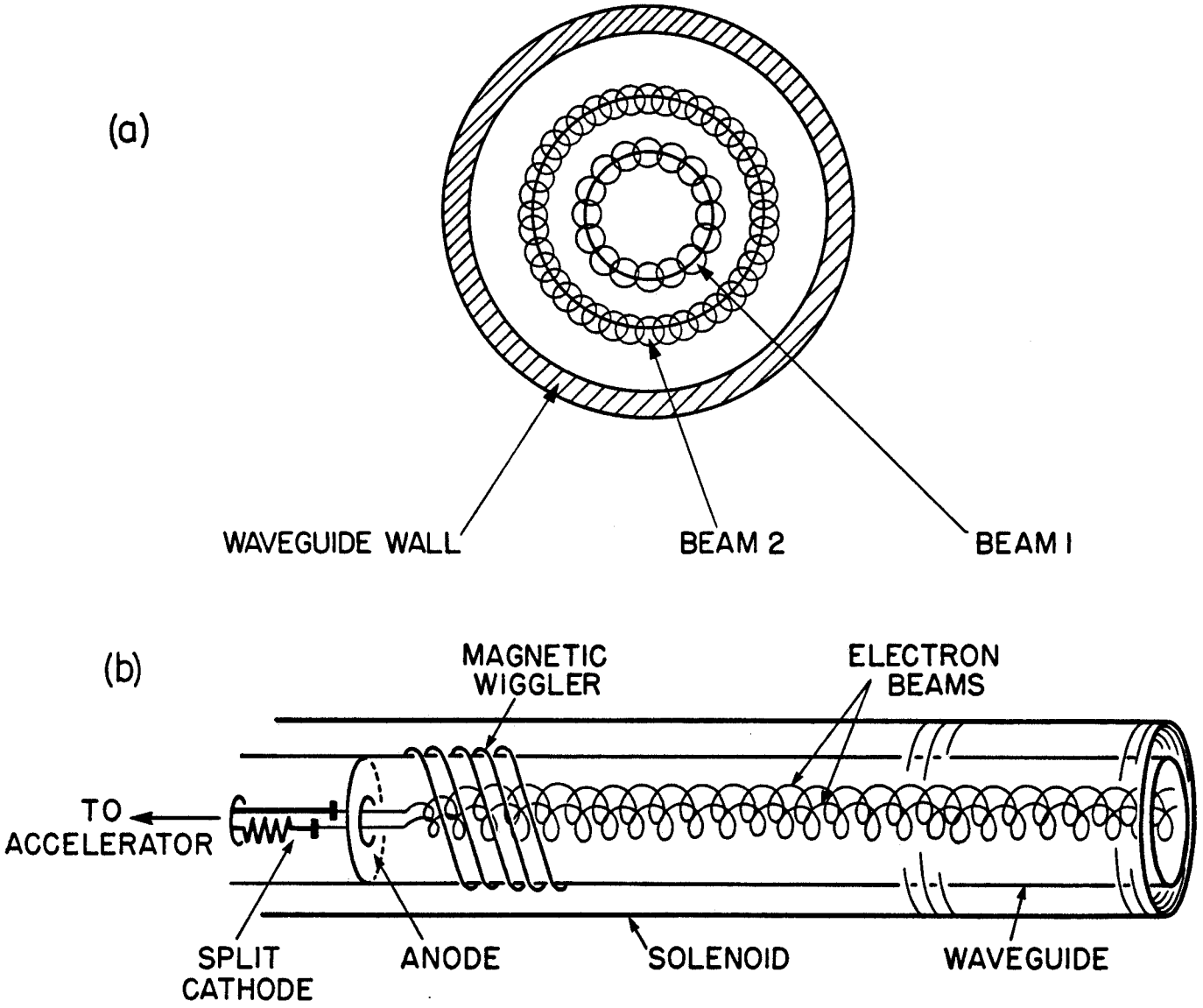
(a)
WAVEGUIDE WALL
BEAM 2
BEAM I
(b)
MAGNETIC WIGGLER
ELECTRON BEAMS
TO ACCELERATOR
SPLIT CATHODE
ANODE
SOLENOID
WAVEGUIDE

Figure 2

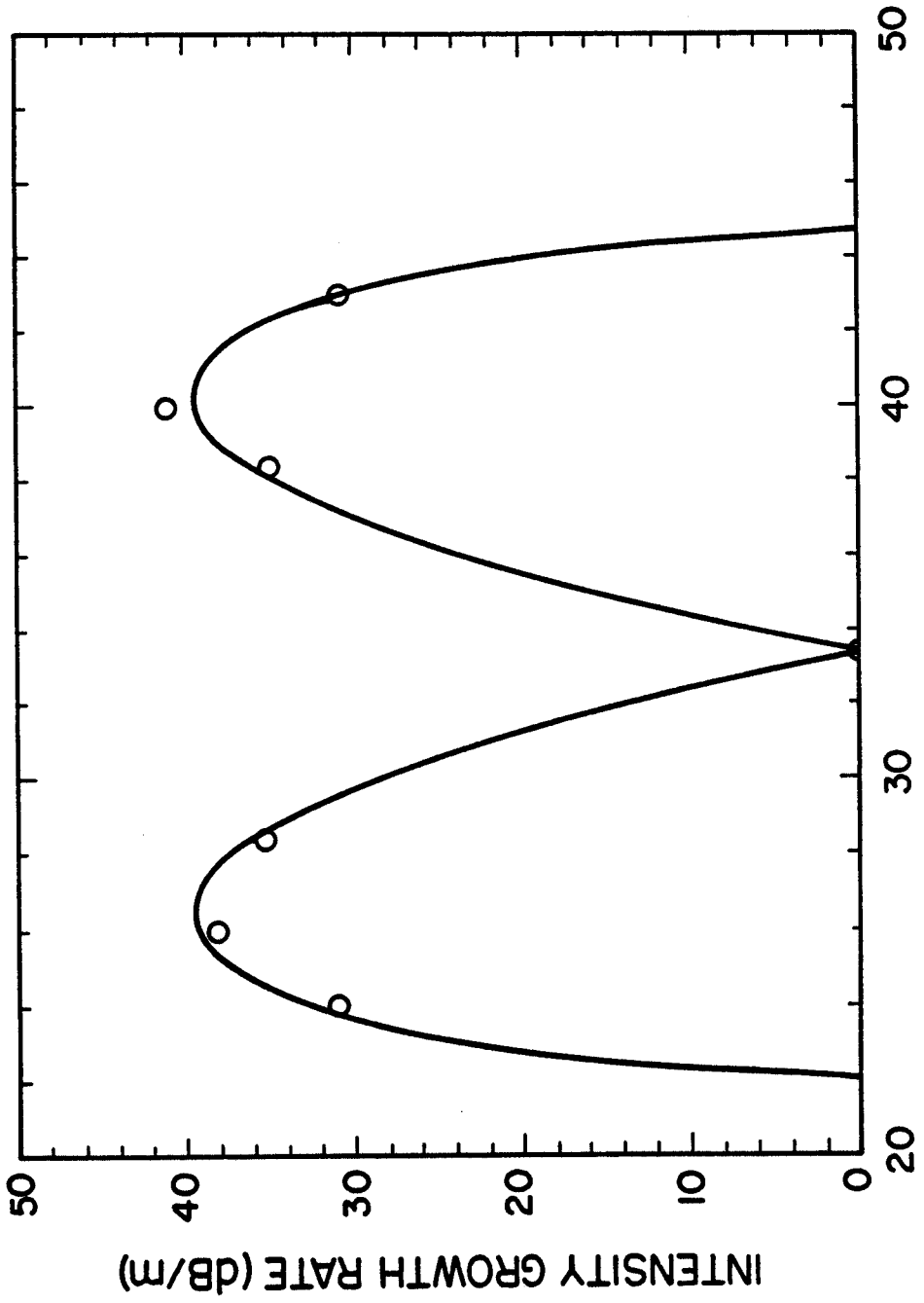
INTENSITY GROWTH RATE (dB/m)
0
10
20
30
40
50
20
30
40
50
FREQUENCY (GHz)

Figure 3

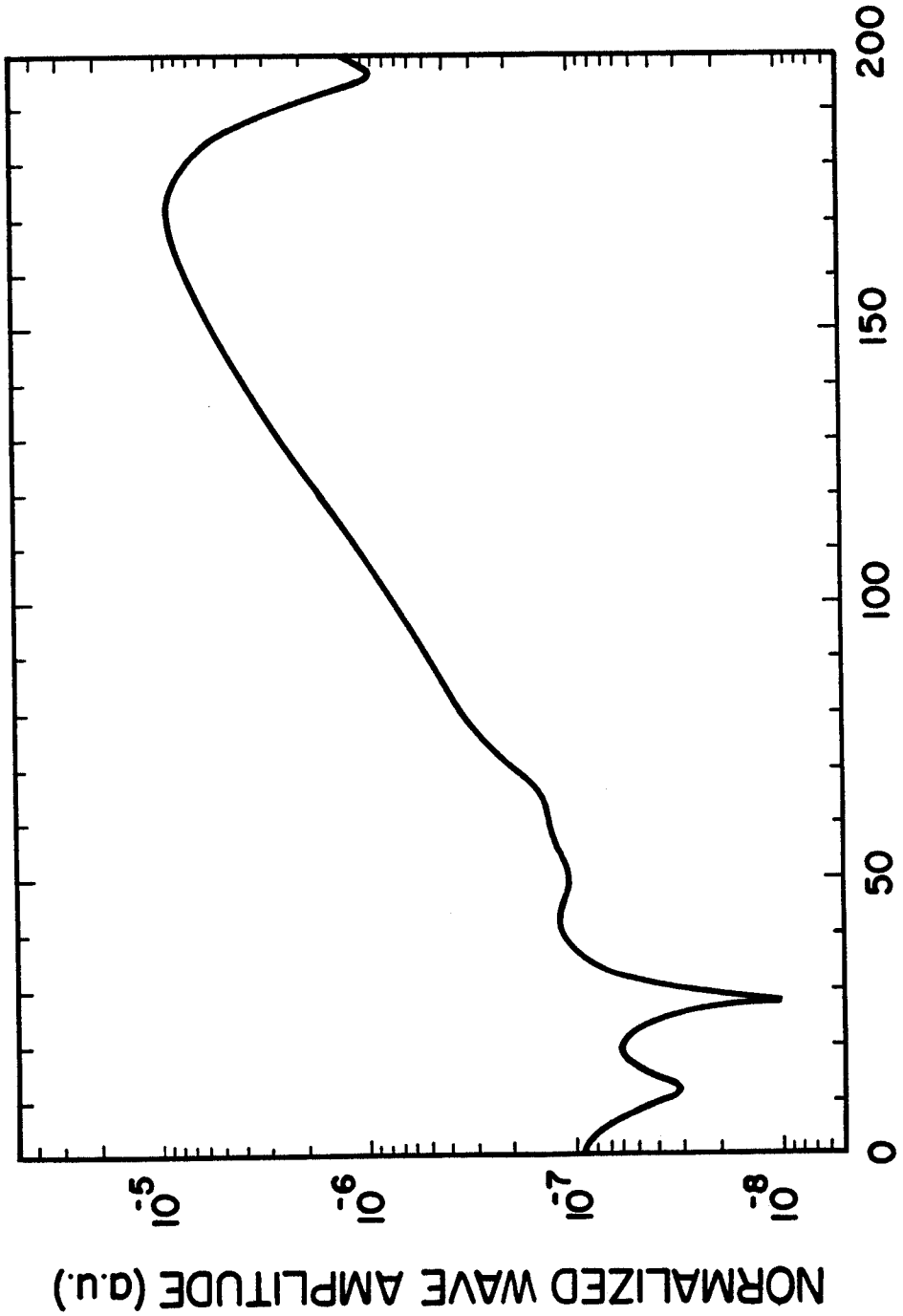
NORMALIZED WAVE AMPLITUDE (a.u.)
10^{-5}
10^{-6}
10^{-7}
10^{-8}
0
50
100
150
200
INTERACTION LENGTH (cm)

Figure 4

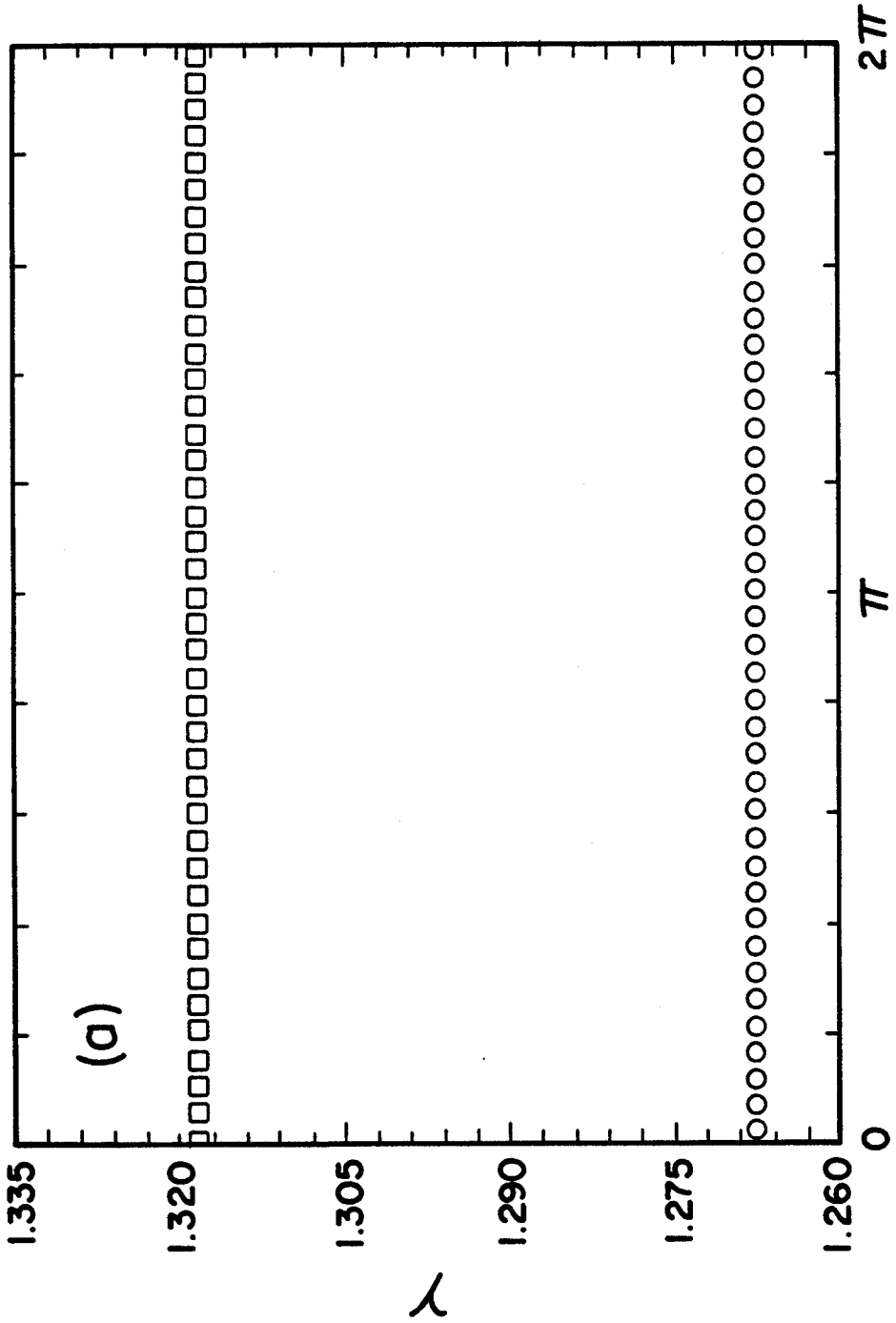

Figure 5(a)

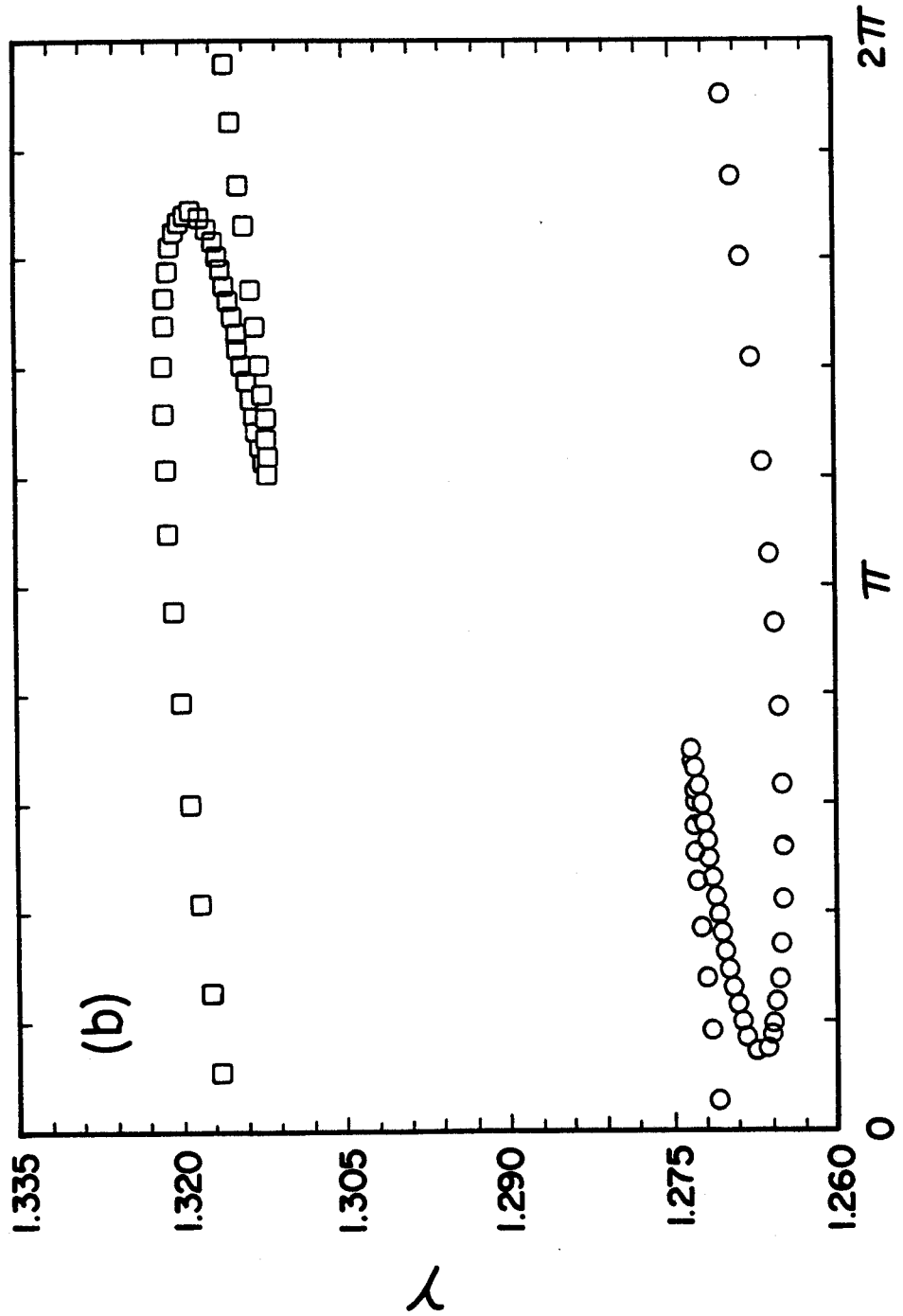

Figure 5(b)

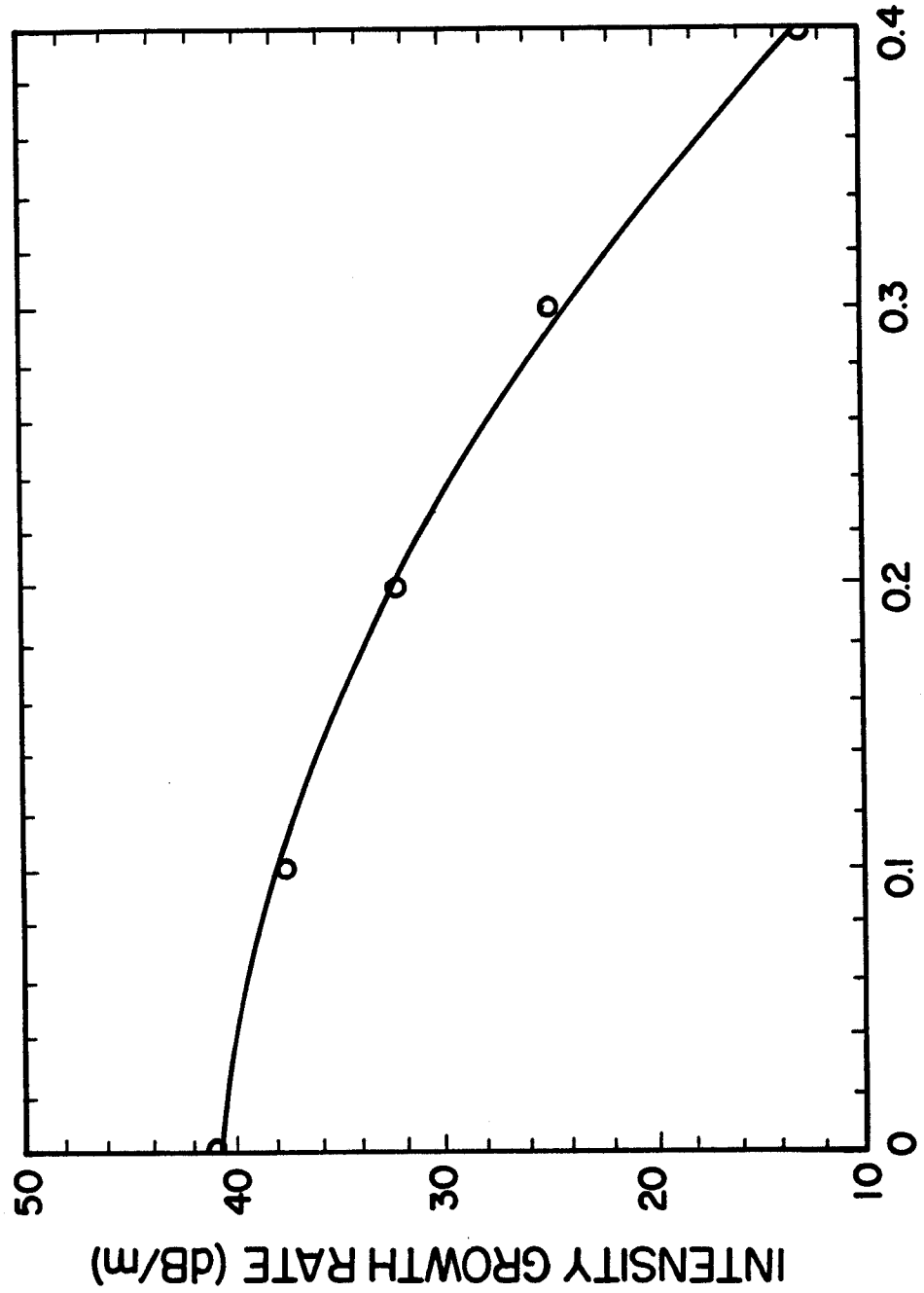
INTENSITY GROWTH RATE (dB/m)
50
40
30
20
10
0
0.1
0.2
0.3
0.4
AXIAL MOMENTUM SPREAD (%)

Figure 6